

## *CHAPTER 4*

# **DIELECTRIC RELAXATION PHENOMENA OF POLYSUBSTITUTED BENZENES UNDER HIGH FREQUENCY ELECTRIC FIELD**

#### 4.1. Introduction :

The dielectric relaxation phenomena of polysubstituted dielectropolar benzenes in benzene under high frequency (*hf*) electric field are of much importance to yield the structural aspect of a polar molecule. There exist several methods [4.1-4.2] to measure relaxation time  $\tau_j$  and dipole moment  $\mu_j$  of a polar molecule (j) from the measured real  $\epsilon_{ij}'$  and imaginary  $\epsilon_{ij}''$  parts of the relative *hf* complex permittivity  $\epsilon_{ij}^*$  of the solution (ij). However, such investigation on the relaxation phenomena of polysubstituted benzenes has not yet been made from the conductivity measurement [4.3-4.4]. Moreover, the most effective dispersive region for such polar liquids may exist at ~10 GHz (X-band) electric field [4.5]. Recently, Paul *et al* [4.6] had measured  $\epsilon_{ij}'$ ,  $\epsilon_{ij}''$  of some polysubstituted benzenes in  $C_6H_6$  at 30<sup>o</sup>, 35<sup>o</sup>, 40<sup>o</sup> and 45<sup>o</sup>C under nearly 10 GHz electric field. The purpose of the study was to see the variation of  $\tau$ 's and  $\mu$ 's with temperature and concentration based on Gopalakrishna's method [4.1].

Although, the molecules appear to be of outdated interest, two polar molecules have identical molecular weights in comparison to the third one, which is slightly higher. One molecule is a para-compound showing zero dipole moment at lower and higher temperatures. The substituted polar groups are attached with the parent benzene ring with different angles. We are, therefore tempted to use the measured relative permittivities [4.6] to get  $\tau_j$  and  $\mu_j$  of these liquids by *hf* conductivity measurement method [4.7]. The methodology is, however, involved with the transfer of dipolar charge of a polar molecule in a given solvent [4.8]. The present method of study in SI unit is superior because of its unified, coherent and rationalised nature. The dependency of  $\tau_j$ 's and  $\mu_j$ 's on *t* in <sup>o</sup>C is of much significance to get an idea of molecular environment and to shed more light on the structural conformations [4.9].

The measured dimensionless dielectric constants like real  $k_{ij}'$  and imaginary  $k_{ij}''$  parts of complex dielectric constant  $k_{ij}^*$  at 30<sup>o</sup>, 35<sup>o</sup>, 40<sup>o</sup> and 45<sup>o</sup>C are placed in Table 4.1. The real  $\sigma_{ij}'$  and imaginary  $\sigma_{ij}''$  parts of the *hf* complex conductivity  $\sigma_{ij}^*$  in  $\Omega^{-1}m^{-1}$  are, however, related to  $k_{ij}''$  and  $k_{ij}'$  respectively.  $\tau_j$ 's are calculated from the linear slope of  $\sigma_{ij}''$  against  $\sigma_{ij}'$  curves [4.10] for different  $w_j$ 's of solute at a given temperature. The variation of  $\sigma_{ij}''$  against  $\sigma_{ij}'$  is not strictly linear for different  $w_j$ 's. (Fig.4.1). The ratio of the individual slopes of variations of  $\sigma_{ij}''$  and  $\sigma_{ij}'$  with  $w_j$ 's in Figs.4.2 and 4.3 in the limit  $w_j=0$  may be used to get  $\tau_j$ 's, in which polar-polar interactions are almost eliminated. All the  $\tau_j$ 's are shown in Table 4.2 and are smaller than the reported  $\tau$ 's [4.6]. We, therefore, recalculated both  $\tau$ 's and  $\mu$ 's based on Gopalakrishna's method [4.1] which are in agreement with those of conductivity measurement. All  $\tau$ 's and  $\mu$ 's are presented in Tables 4.2 and 4.4 respectively for comparison.

Thermodynamic energy parameters: enthalpy of activation  $\Delta H_\tau$ , free energy of activation  $\Delta F_\tau$  and entropy of activation  $\Delta S_\tau$  for dielectric relaxations are also computed from the slope and intercept of  $\ln(\tau_j T)$  against  $1/T$  of Fig.4.4 with  $\tau_j$ 's measured by both the methods [4.11]. The values are entered in Table 4.3 in order to infer molecular dynamics of polar molecules in benzene. The enthalpy of activation  $\Delta H_\eta$  for viscous process was, however, obtain from the linear slope  $\gamma$  of  $\ln(\tau_j T)$  against  $\ln \eta$  and  $\Delta H_\tau$  of Eq.(4.4). The coefficients of viscosity  $\eta$  of solvent  $C_6H_6$  are  $5.65 \times 10^{-3}$ ,  $5.30 \times 10^{-3}$ ,  $5.03 \times 10^{-3}$  and  $4.70 \times 10^{-3}$  poise at  $30^\circ$ ,  $35^\circ$ ,  $40^\circ$  and  $45^\circ C$  respectively.

Table 4.1: The real and imaginary parts of dimensionless dielectric constants of different aromatic polar liquids in benzene for different weight fractions  $w_j$ 's at various experimental temperatures in  $^\circ C$ .

Weight fraction $w_j$	$k_{ij}'$	$k_{ij}''$	$k_{ij}'$	$k_{ij}''$	$k_{ij}'$	$k_{ij}''$	$k_{ij}'$	$k_{ij}''$
	30 $^\circ C$		35 $^\circ C$		40 $^\circ C$		45 $^\circ C$	
(I) meta-diisopropylbenzene								
0.012	2.2990	0.0424	2.3062	0.0401	2.3151	0.0393	2.3271	0.0384
0.018	2.3323	0.0570	2.3425	0.0552	2.3541	0.0545	2.3660	0.0523
0.025	2.3614	0.0721	2.3711	0.0692	2.3923	0.0660	2.4105	0.0595
0.032	2.3852	0.1083	2.4084	0.0985	2.4212	0.0854	2.4462	0.0734
0.045	2.4104	0.1251	2.4234	0.1092	2.4451	0.0982	2.4671	0.0832
(II) para-methylbenzoylchloride								
0.011	2.1603	0.0488	2.1663	0.0440	2.1723	0.0410	2.1783	0.0381
0.018	2.1960	0.0585	2.2018	0.0553	2.2078	0.0523	2.2140	0.0492
0.028	2.2351	0.0690	2.2411	0.0662	2.2470	0.0632	2.2530	0.0603
0.039	2.2754	0.0762	2.2812	0.0731	2.2872	0.0701	2.2931	0.0672
0.050	2.3089	0.0928	2.3147	0.0899	2.3204	0.0872	2.3263	0.0842
(III) ortho-chloroacetophenone								
0.011	2.1843	0.0351	2.1861	0.0330	2.1901	0.0310	2.1982	0.0294
0.023	2.2198	0.0462	2.2322	0.0442	2.2394	0.0450	2.2456	0.0376
0.032	2.2590	0.0573	2.2698	0.0552	2.2700	0.0491	2.2801	0.0421
0.045	2.2991	0.0692	2.3002	0.0653	2.3204	0.0551	2.3324	0.0579
0.051	2.3323	0.0810	2.3452	0.0791	2.3612	0.0770	2.3711	0.0650

Dipole moments  $\mu_j$ 's (shown in Table 4.4) are estimated from the linear coefficients  $\beta$ 's of  $hf \sigma_{ij}$  against  $w_j$ 's as displayed in Fig.4.5 in the limit  $w_j=0$ . The variation of  $\mu_j$ 's and  $\tau_j$ 's with  $t$  in  $^\circ C$  are presented in Fig.4.6. The temperature dependence of the mesomeric and inductive moments of the substituted polar groups attached to the parent molecules [4.12] are taken into account to display the theoretical dipole moments  $\mu_{theo}$ 's in Fig.4.7.

Table 4.2: The slope of linear relation  $\sigma_{ij}''-\sigma_{ij}'$  curves of Fig. 4.1, correlation coefficient 'r', % of errors in regression technique, ratio of slopes of  $\sigma_{ij}''-w_j$  and  $\sigma_{ij}'-w_j$  curves at  $w_j \rightarrow 0$  of Figs.4.2 and 4.3, estimated  $\tau_j$  from Eq.(4.2) and reported  $\tau$  in psec.

System with sl. no.	$t$ in $^{\circ}\text{C}$	Slope of $\sigma_{ij}''-\sigma_{ij}'$ curve of Eq.(4.2)	'r'	% of error of Eq.(4.2)	Ratio of slopes of $\sigma_{ij}''-w_j$ & $\sigma_{ij}'-w_j$ at $w_j \rightarrow 0$	$\tau_j^a$	$\tau_j^b$	Rept. $\tau$ in psec.
(I) m-diisopropylbenzene in $\text{C}_6\text{H}_6$	30	1.217	0.972	1.67	1.809	13.08	8.80	10.92
	35	1.633	0.990	0.60	2.173	9.75	7.33	8.88
	40	2.183	0.990	0.60	2.916	7.29	5.46	6.54
	45	3.227	0.988	0.72	4.207	4.93	3.79	4.30
(II) p-methylbenzoylchloride in $\text{C}_6\text{H}_6$	30	3.491	0.988	0.72	5.858	4.56	2.72	3.85
	35	3.369	0.989	0.66	4.828	4.73	3.30	4.04
	40	3.342	0.988	0.72	4.931	4.77	3.23	4.05
	45	3.339	0.988	0.72	4.910	4.77	3.24	4.18
(III) o-chloroacetophenone in $\text{C}_6\text{H}_6$	30	3.268	0.999	0.06	3.793	4.87	4.20	4.43
	35	3.406	0.998	0.12	5.234	4.68	3.04	4.16
	40	3.841	0.963	2.19	12.625	4.15	1.26	3.47
	45	4.614	0.987	0.78	17.625	3.45	0.90	3.09

$\tau_j^a$  = Estimated relaxation time from Eq.(4.2) with slope of  $\sigma_{ij}''-\sigma_{ij}'$ .

$\tau_j^b$  = Estimated relaxation time from Eq.(4.2) with ratio of slopes of  $\sigma_{ij}''-w_j$  and  $\sigma_{ij}'-w_j$  at  $w_j \rightarrow 0$ .

#### 4.2. Theoretical Formulation :

Under electric field of giga hertz range the  $hf$  complex conductivity  $\sigma_{ij}^*$  of polar-nonpolar liquid mixture is :

$$\sigma_{ij}^* = \omega \epsilon_o k_{ij}'' + j \omega \epsilon_o k_{ij}' \quad \dots (4.1)$$

where  $\omega \epsilon_o k_{ij}' (= \sigma_{ij}'')$  and  $\omega \epsilon_o k_{ij}'' (= \sigma_{ij}')$  are the imaginary and real parts of  $\sigma_{ij}^*$ .  $\omega (= 2\pi f)$  is the angular frequency of the applied electric field of frequency  $f$ .  $\epsilon_o =$  permittivity of free space =  $8.854 \times 10^{-12} \text{ F.m}^{-1}$  and  $j$  is a complex number  $= \sqrt{-1}$ . The magnitude of total  $hf$  conductivity is :

$$\sigma_{ij} = \omega \epsilon_o (k_{ij}''^2 + k_{ij}'^2)^{1/2}$$

$\sigma_{ij}'$  and  $\sigma_{ij}''$  of a given weight fraction  $w_j$  are, however, related to  $\tau_j$  by :

$$\sigma_{ij}'' = \sigma_{\infty ij} + \frac{1}{\omega \tau_j} \sigma_{ij}'$$

$$\left( \frac{d\sigma_{ij}''}{d\sigma_{ij}'} \right)_{w_j \rightarrow 0} = \frac{(d\sigma_{ij}''/dw_j)_{w_j \rightarrow 0}}{(d\sigma_{ij}'/dw_j)_{w_j \rightarrow 0}} = \frac{1}{\omega \tau_j} \quad \dots (4.2)$$

The variation of  $\sigma_{ij}''$  against  $\sigma_{ij}'$  for different  $w_j$ 's is not always linear as shown in Fig.4.1. In such case, one may use the ratio of the individual slopes of variations of  $\sigma_{ij}''$  and  $\sigma_{ij}'$  against  $w_j$ 's as seen in Figs.4.2 and 4.3 in the limit  $w_j=0$  to get  $\tau_j$ .

Table 4.3: Thermodynamic energy parameters: enthalpy of activation  $\Delta H_\tau$ , entropy of activation  $\Delta S_\tau$  and free energy of activation  $\Delta F_\tau$ , value of  $\gamma$  from Eq.(4.4), enthalpy of activation  $\Delta H_\eta$  due to viscous process, Debye factor and Kalman factor of the following aromatic polar liquids in benzene at different temperatures.

System with sl. no.	$t$ in $^{\circ}\text{C}$	$\Delta H_\tau$ in K J mole $^{-1}$	$\Delta S_\tau$ in J mole $^{-1}$ K $^{-1}$	$\Delta F_\tau$ in K J mole $^{-1}$	Value of $\gamma$ from Eq.(4.4)	$\Delta H_\eta$ from $\Delta H_\eta = \Delta H_\tau / \gamma$ in K J mole $^{-1}$	Debye factor $(\tau_j T / \eta) \times 10^7$	Kalman Factor $\tau_j T / \eta^\gamma$
(I) m-diisopropylbenzene in $\text{C}_6\text{H}_6$	30		106.96	10.11			4.72	11.74
	35	42.52	106.07	9.85	4.29	9.91	4.26	13.08
	40		106.17	9.29			3.40	12.39
	45		106.94	8.51			2.56	11.69
(II) p-methylbenzoylchloride in $\text{C}_6\text{H}_6$	30		-59.41	7.16				
35	-10.84	-60.57	7.82	-1.10	9.85	1.92	$3.19 \times 10^{-12}$	
40		-59.96	7.93			2.01	$3.00 \times 10^{-12}$	
45		-59.58	8.11			2.19	$2.83 \times 10^{-12}$	
(III) o-chloroacetophenone in $\text{C}_6\text{H}_6$	30		255.28			8.25		
35	85.60	253.25	7.60	8.73	9.81	1.77	$6.89 \times 10^{10}$	
40		255.99	5.48			0.78	$4.58 \times 10^{10}$	
45		254.36	4.71			0.61	$6.02 \times 10^{10}$	

$\tau_j$ 's by both the methods of  $(d\sigma_{ij}''/d\sigma_{ij}')$  and the ratio of individual slopes of Eq.(4.2) are used to get free energy of activation  $\Delta F_\tau$  of a polar liquid. From Eyring's rate theory [4.11] one gets:

$$\ln(\tau_j T) = \ln(Ae^{-\Delta S_\tau/R}) + \Delta H_\tau / RT \quad \dots (4.3)$$

Since  $\Delta F_\tau = \Delta H_\tau - T\Delta S_\tau$

The intercept and slope of  $\ln(\tau_j T)$  against  $1/T$  as shown in Fig.4.4 are, however, related to  $\Delta S_\tau$  and  $\Delta H_\tau$  of molecules.  $\eta$  of  $\text{C}_6\text{H}_6$  is related to  $\tau_j$  at different temperatures by:

$$\tau_j = A\eta^\gamma / T \quad \dots (4.4)$$

Where  $\gamma$  is the slope of the linear relation of  $\ln(\tau_j T)$  against  $\ln \eta$ . Again,  $\sigma_{ij}''$  may be approximated to  $\sigma_{ij}$  for their identical nature of variations with  $w_j$ 's as evidenced by Figs.4.2 and 4.5 respectively.

Hence Eq.(4.2) can be written as :

$$\sigma_{ij}'' = \sigma_{\infty ij} + \frac{1}{\omega \tau_j} \sigma_{ij}'$$

$$\left( \frac{d\sigma'_{ij}}{dw_j} \right)_{w_j \rightarrow 0} = \beta \omega \tau_j \quad \dots (4.5)$$

where  $\beta$  is the linear coefficient of variation of  $\sigma_{ij}-w_j$  curves of Fig.4.5 at  $w_j \rightarrow 0$ . All  $\beta$ 's are placed in Table 4.4. The real part  $\sigma'_{ij}$  at TK is [4.13]:

$$\sigma'_{ij} = \frac{N\rho_i\mu_j^2}{27k_B TM_j} \left( \frac{\omega^2 \tau_j}{1 + \omega^2 \tau_j^2} \right) (k'_{ij} + 2)^2 w_j$$

$$\left( \frac{d\sigma'_{ij}}{dw_j} \right)_{w_j \rightarrow 0} = \frac{N\rho_i\mu_j^2}{27k_B TM_j} \left( \frac{\omega^2 \tau_j}{1 + \omega^2 \tau_j^2} \right) (k_i + 2)^2 \quad \dots (4.6)$$

where  $N$ =Avogadro's number,  $\rho_i$ =density of solvent,  $k_i$ =dimensionless dielectric constant of solvent,  $M_j$ =molecular weight of the polar liquid (j) and  $k_B$ =Boltzmann constant. All the symbols are in SI units. From Eqs.(4.5) and (4.6) one gets  $\mu_j$  of a polar molecule in Coulomb metre (C.m):

$$\mu_j = \left( \frac{27k_B TM_j}{N\rho_i (k_i + 2)^2} \frac{\beta}{\omega b} \right)^{1/2} \quad \dots (4.7)$$

The dimensionless parameter  $b$  is related to  $\tau_j$  by :

$$b = \frac{1}{1 + \omega^2 \tau_j^2} \quad \dots (4.8)$$

The measured  $\tau_j$ 's of the polar liquids presented in Table 4.2 are compared with the recalculated  $\tau$ 's based on Gopalakrishna's [4.1] method.

$$x = \frac{\varepsilon_{ij}'^2 + \varepsilon_{ij}' + \varepsilon_{ij}''^2 - 2}{(\varepsilon_{ij}' + 2)^2 + \varepsilon_{ij}''^2} \quad y = \frac{3\varepsilon_{ij}''}{(\varepsilon_{ij}' + 2)^2 + \varepsilon_{ij}''^2}$$

$$\tau = \frac{1}{\omega} \frac{dy}{dx} \quad \dots (4.9)$$

All the  $\mu_j$ 's with  $b$ 's are finally found in Table 4.4 to compare with recalculated  $\mu$ 's from :

$$\mu = \left[ \frac{9k_B TM_j}{4\pi N\rho_i} \left\{ 1 + \left( \frac{dy}{dx} \right)^2 \right\} \frac{dx}{dw_j} \right]^{1/2} \quad \dots (4.10)$$

All the computed  $\mu_j$ 's reported  $\mu$ 's along with  $\mu_{theo}$ 's of Fig.4.7 are seen in Table 4.4.

### 4.3. Results and Discussions :

The relaxation times  $\tau_j$ 's of polysubstituted benzenes under 3 cm wavelength electric field, were calculated simultaneously from Eq.(4.2) with the slope of  $\sigma_{ij}''$  against  $\sigma_{ij}'$  of  $hf$  conductivity  $\sigma_{ij}^*$  of Fig.4.1 and the ratio of slopes of the variations of  $\sigma_{ij}''$  and  $\sigma_{ij}'$  with  $w_j$ 's of Figs.4.2 and 4.3 from data of Table 4.1 at different experimental temperatures.  $\tau_j$ 's (Table 4.2) from slope of linear relation  $\sigma_{ij}''-\sigma_{ij}'$  curve (Fig.4.1) are slightly larger than the ratio of slopes of Eq.(4.2). The latter

method is reliable as the polar-polar interactions are almost eliminated. The variation of  $\sigma_{ij}''$  with  $\sigma_{ij}'$  is non linear (Fig.4.1) for all the liquids like  $\sigma_{ij}''$  and  $\sigma_{ij}'$  with  $w_j$ 's of Figs.4.2 & 4.3 respectively. The slopes of curves in Fig.4.1 are almost same for *p*-methylbenzoylchloride, but for *o*-chloroacetophenone the curves are of almost constant intercepts and slightly increasing slopes with temperature to yield almost same  $\tau_j$  for their same polarity [4.14] and identical structures. Meta-diisopropylbenzene indicates the lower intercept and higher slopes as the temperature rises.  $\tau_j$ 's from Eq.(4.2) of  $\sigma_{ij}''-\sigma_{ij}'$  curves decrease with temperature to obey Debye

relaxation mechanism like the variation of  $\sigma_{ij}''$  and  $\sigma_{ij}'$  with  $w_j$ 's for the molecules at 30<sup>o</sup>, 35<sup>o</sup>, 40<sup>o</sup> and 45<sup>o</sup>C respectively. Nevertheless, the conductivity method yields microscopic  $\tau_j$ 's [4.15]. The molecule *m*-diisopropylbenzene has greater  $\tau$  because of larger size than those of isomeric *p*-methylbenzoylchloride and *o*-chloroacetophenone.  $\tau_j$ 's in Table 4.2 for these molecules having the same number of C-atoms do not vary much from Eqs.(4.2) and (4.9) respectively probably for the different positions of the substituted polar groups attached to the parent molecules of Fig.4.7.

For *m*-diisopropylbenzene both  $\sigma_{ij}''$  and  $\sigma_{ij}'$  in Figs.4.2 and 4.5 start from 1.228  $\Omega^{-1}m^{-1}$  to 1.236  $\Omega^{-1}m^{-1}$  and increase gradually to assume maximum within  $0.045 \leq w_j \leq 0.051$  and then decrease as  $w_j$  increases. This sort of behaviour arises for the transfer of localised charge species of

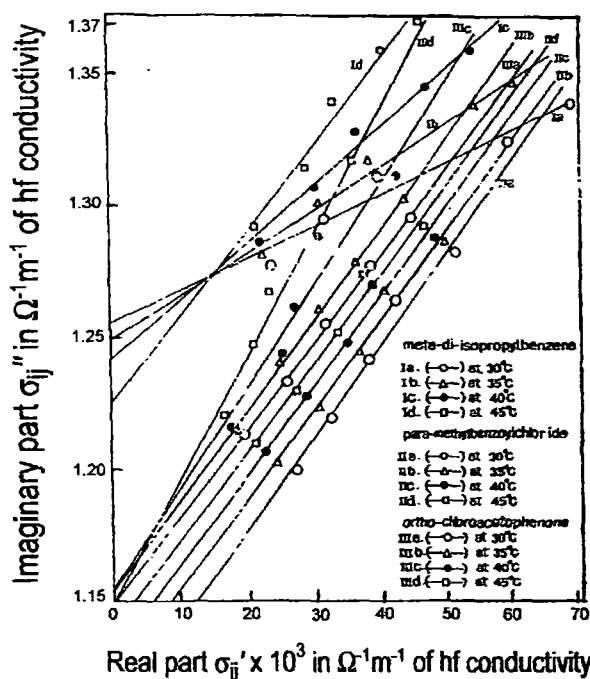


Figure 4.1: Variation of imaginary part  $\sigma_{ij}''$  in  $\Omega^{-1}m^{-1}$  against real part  $\sigma_{ij}'$  in  $\Omega^{-1}m^{-1}$  of  $hf$  conductivity for different weight fractions  $w_j$ 's of polysubstituted benzenes in benzene under 10 GHz electric field at various experimental temperatures.

such dipoles [4.16] which increases up to a certain  $w_j$  and then ceases gradually in the higher concentrations. Similar observation is noted in *p*-methylbenzoylchloride showing maximum at nearly  $w_j=0.096$ . All these facts indicate the phase transition of lower conductivity in the higher concentration [4.16] probably due to dimer formations. Ortho-chloroacetophenone showed a regular monotonic increase, as coefficients of quadratic term of  $w_j$  in both  $\sigma_{ij}''$  and  $\sigma_{ij}$  are positive. The variation of  $\sigma_{ij}'$  with  $w_j$ 's for all polar molecules in Fig.4.3 decreases with  $t$  °C to exhibit the

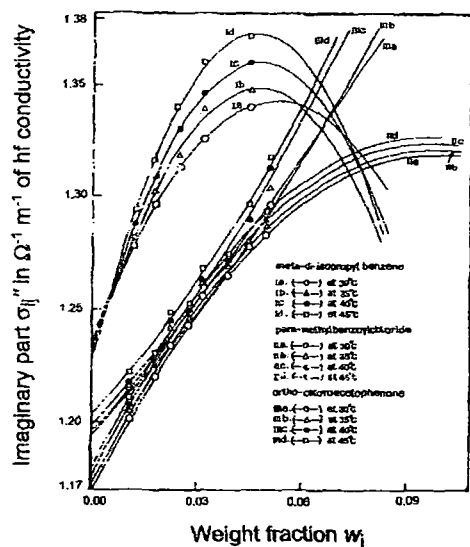


Figure 4.2: Variation of imaginary part  $\sigma_{ij}''$  in  $\Omega^{-1} \text{m}^{-1}$  of hf conductivity with weight fractions  $w_j$ 's of polysubstituted benzenes in benzene under 10 GHz electric field.

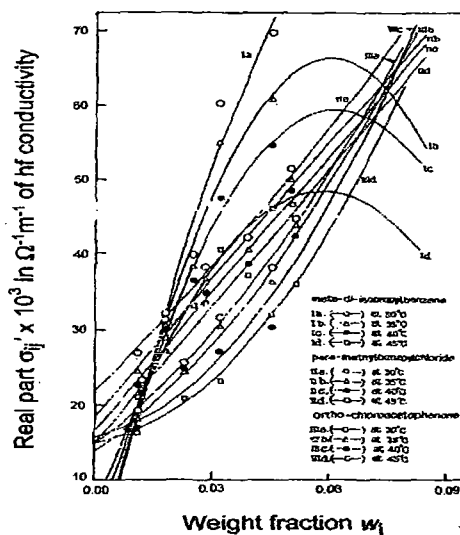


Figure 4.3: Variation of real part  $\sigma_{ij}'$  in  $\Omega^{-1} \text{m}^{-1}$  of hf conductivity with weight fractions  $w_j$ 's of polysubstituted benzenes in benzene under 10 GHz electric field.

semiconducting nature while  $\sigma_{ij}''$  and  $\sigma_{ij}$  of Figs.4.2 and 4.5 showed the regular increase. The percentage of errors as well as correlation coefficients  $r$ 's are made for Eq.(4.2) to get  $\tau_j$ 's. It is interesting to note that  $\tau_j$  for *m*-diisopropylbenzene and *o*-chloroacetophenone in  $\text{C}_6\text{H}_6$  obey Debye relaxation mechanism. The energy difference between activated and normal states of the random dipole orientations increases with  $t$  °C to decrease  $\tau_j$ 's.  $\tau_j$ 's for *p*-methylbenzoylchloride initially increases and then become constant with  $t$  °C indicating the non-Debye relaxation for its asymmetry gained by two polar groups in a line. The large difference between  $\tau_j$ 's and reported  $\tau$ 's [4.6] prompted us to recalculate  $\tau$ 's placed in the 9th column of Table 4.2 based on Gopalakrishna's method [4.1]. The recalculated  $\tau$ 's and  $\mu$ 's are now closer to  $\tau_j$ 's of columns 7 and 8 of Table 4.2 and  $\mu_j$ 's of column 9 of Table 4.4 based on the method of conductivity measurement [4.7].

The thermodynamic energy parameters  $\Delta H_\tau$ ,  $\Delta S_\tau$  and  $\Delta F_\tau$  (Table 4.3) were calculated from  $\ln(\tau_j T)$  against  $1/T$  in Fig.4.4 with the measured  $\tau_j$ 's by both the methods. In *p*-

methylbenzoylchloride  $-\Delta S_r$  indicates the activated states are more stable supported by  $-\Delta H_r$  also.  $\Delta S_r$  for *m*-diisopropylbenzene and *o*-chloroacetophenone indicates the unstability of the activated

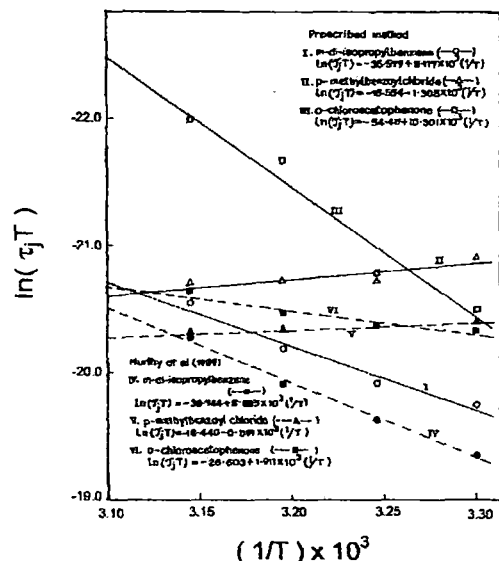


Figure 4.4: The linear plot of  $\ln(\tau_j T)$  against  $1/T$

Kalman factors being proportional to the volumes of the rotating units are of different orders, but constant with temperature for a given system. Debye factors, on the other hand, are of the order of  $10^{-7}$  for all systems. This suggests the applicability of Debye-Smyth model of dielectric relaxation mechanism for all the liquids including *p*-methylbenzoylchloride although it is non-Debye in

Table 4.4: The coefficients of *hf* conductivity  $\sigma_{ij}$  of aromatic polar liquid with weight fraction  $w_j$  in  $C_6H_6$  at  $30^\circ$ ,  $35^\circ$ ,  $40^\circ$  and  $45^\circ C$  in Fig.4.5, dimensionless parameters *b*'s, computed, reported and theoretical dipole moments in Coulomb metre (C.m).

System with sl. no & mol. wt.	<i>t</i> in $^\circ C$	Coefficients of $\sigma_{ij}-w_j$ in $\Omega^{-1}m^{-1}$ of Fig.4.5 $\sigma_{ij} = \alpha + \beta w_j + \xi w_j^2$			Dimensionless parameter <i>b</i>	Computed $\mu_j \times 10^{30}$ in C.m		Rept. $\mu \times 10^{30}$ in C.m Eq.(4.10)	$\mu_{theo} \times 10^{30}$ in C.m of Fig.4.7	
		$\alpha$	$\beta$	$\xi$						
(I) <i>m</i> -diisopro- pylbenzene in $C_6H_6$ $M_j=0.162$ Kg	30	1.236	4.016	-36.919	0.597	0.766	14.34	12.66	9.07	3.77
	35	1.228	5.110	-53.613	0.727	0.825	14.86	13.95	8.90	
	40	1.230	5.475	-56.900	0.827	0.895	14.61	14.04	8.84	
	45	1.228	6.196	-65.944	0.913	0.946	14.99	14.72	8.90	
(II) <i>p</i> -methyl- benzoylchloride in $C_6H_6$ $M_j=0.156$ Kg	30	1.171	3.059	-15.421	0.924	0.972	9.87	9.63	8.17	8.80
	35	1.173	3.059	-15.464	0.919	0.959	10.03	9.82	8.27	
	40	1.177	3.064	-15.617	0.918	0.961	10.18	9.95	8.34	
	45	1.180	3.064	-15.685	0.918	0.960	10.31	10.08	8.44	
(III) <i>o</i> -chloro- acetophenone in $C_6H_6$ $M_j=0.156$ Kg	30	1.197	1.477	9.038	0.915	0.935	6.90	6.82	8.07	7.40
	35	1.195	1.894	3.180	0.921	0.965	7.89	7.71	8.20	
	40	1.201	1.580	11.513	0.936	0.994	7.23	7.02	8.57	
	45	1.204	1.615	11.737	0.955	0.997	7.34	7.19	8.74	

states. Unlike *p*-methylbenzoylchloride,  $\gamma > 0.5$  for *m*-diisopropylbenzene and *o*-chloroacetophenone indicates that they do not behave as solid phase rotators. Such polar liquids in  $C_6H_6$  favour solute-solvent molecular formation.  $\Delta H_r$  involved with translational and rotational energy are less than  $\Delta H_r$  due to high values of  $\gamma$  for all the systems. They thus need maximum energy to rotate under *hf* electric field. The  $\gamma$ 's from the slope of  $\ln(\tau_j T)$  against  $\ln \eta$  are used to estimate Kalman factor  $\tau_j T / \eta^\gamma$  and Debye factor  $\tau_j T / \eta$  to place them in Table 4.3.

relaxation behaviour.  $\mu_j$ 's of the polar liquids at  $t$  °C are estimated from  $\beta$ 's of  $\sigma_{ij}-w_j$  curves of Fig.4.5 and dimensionless parameters  $b$ 's of Eq.(4.8) involved with the measured  $\tau_j$ 's from the ratio of the individual slopes of Figs.4.2 and 4.3 at  $w_j \rightarrow 0$ . The  $\sigma_{ij}$  in  $\Omega^{-1}\text{m}^{-1}$  when plotted with  $w_j$ 's increases with temperatures showing maximum at a certain  $w_j$  for *m*-diisopropylbenzene and *p*-methylbenzoylchloride like  $\sigma_{ij}''-w_j$  curves. This signifies the phase transition from higher to lower conductivity for transfer of charged species of molecules. The slopes and intercepts of  $\sigma_{ij}-w_j$  and  $\sigma_{ij}''-w_j$  curves for *p*-methylbenzoylchloride and *o*-chloroacetophenone are almost the same for their same polarity [4.14] indicating  $\sigma_{ij} \approx \sigma_{ij}''$  in Eq.(4.5). The usual variations of  $\mu_j$  and  $\tau_j$  [4.17] with  $t$  °C

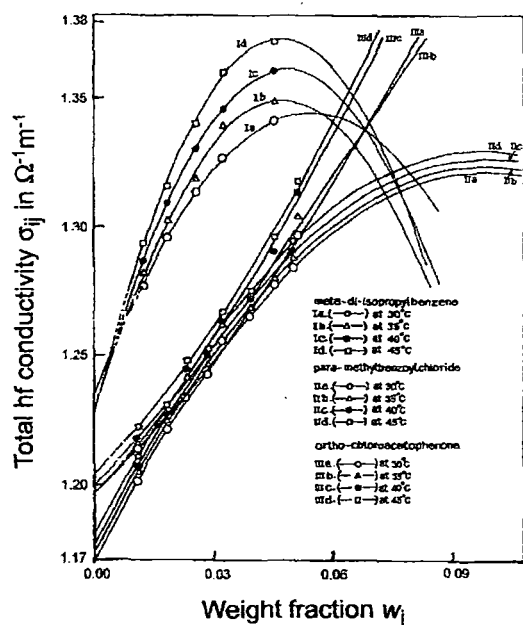


Figure 4.5: Variation of total hf conductivity  $\sigma_{ij}$  in  $\Omega^{-1}\text{m}^{-1}$  with weight fractions  $w_j$ 's under 10 GHz electric field at various experimental temperatures

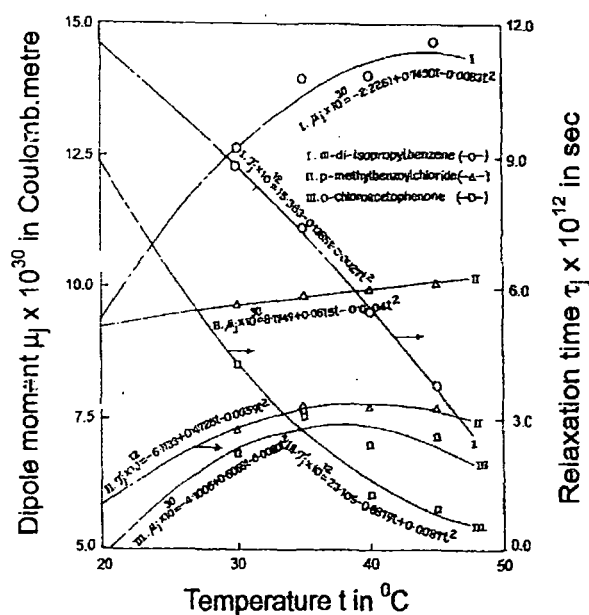


Figure 4.6: Variation of observed dipole moment  $\mu_j$  and relaxation time  $\tau_j$  with temperatures  $t$  in °C of different polysubstituted benzenes in benzene under 10 GHz electric field.

are shown graphically in Fig.4.6.  $\tau_j$ 's decrease with temperature for the curves I and III of *m*-diisopropylbenzene and *o*-chloroacetophenone. The  $\mu_j$ 's from Eq.(4.7) increase gradually to maximum  $14.49 \times 10^{-30}$  C.m at  $44.88$  °C,  $10.54 \times 10^{-30}$  C.m at  $76.88$  °C and  $7.41 \times 10^{-30}$  C.m at  $37.93$  °C respectively signifying the largest asymmetry gained by all the molecules.  $\tau_j$ 's are zero at  $54.03$  °C for the curve I and  $16.22$  °C,  $63.88$  °C for curve II. But for curve III;  $\tau_j = 0$  at  $t = \infty$ . The  $\mu_j$ 's are  $13.80 \times 10^{-30}$  C.m for the curve I and  $9.07 \times 10^{-30}$  C.m,  $10.47 \times 10^{-30}$  C.m for curve II. But undefined for curve III respectively. The variation of  $\tau_j$  and  $\mu_j$  with  $t$  °C are convex for curve II indicating the non-

Debye relaxation behaviour to reveal solute-solvent molecular association as observed from  $\gamma$  of Table 4.3.

$\mu_{theo}$  from the available bond angles and bond moments of the substituted polar groups of molecules of Fig.4.7 is placed in Table 4.4 with the reported  $\mu$  from Eq.(4.10). The close agreement

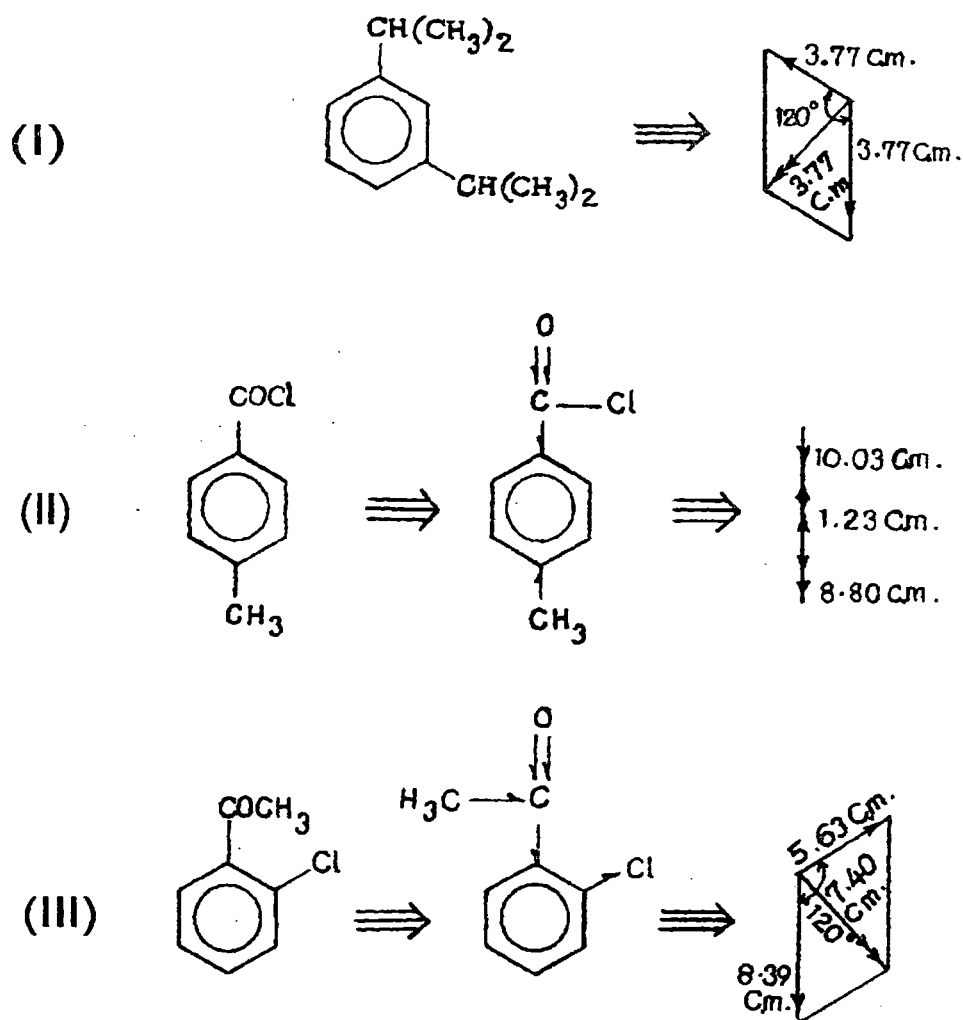


Figure 4.7: Conformational structures of (I) meta-diisopropylbenzene (II) para-methylbenzoylchloride (III) ortho-chloroacetophenone.

of  $\mu_j$ 's of Eq.(4.7) with Eq.(4.10) suggests the basic soundness of the present method. The wide disagreement between  $\mu_j$  and  $\mu_{theo}$  of Table 4.4 of the first molecule unlike the latter two suggest bond moments of the substituted polar groups are either stretched by a factor  $\mu_j/\mu_{theo}$  of 3.36, 3.70, 3.72, 3.90; or shortened by 0.09, 1.12, 1.13, 1.50 and 0.92, 1.04, 0.95, 0.97 respectively in order to consider inductive and mesomeric effects in them. The electromeric effect caused by  $>C=O$  in second and third molecules may be the reason to make  $\mu_j$  more closer to  $\mu_{theo}$  [4.18].

#### 4.4. Conclusion :

The study of dielectric relaxation phenomena of polysubstituted benzenes in benzene under 3 cm wavelength electric field in terms of  $\tau_j$ 's and  $\mu_j$ 's in SI units at various experimental temperatures in  $^{\circ}\text{C}$  by the method of *hf* conductivity measurement is more topical and significant. The use of ratio of the slopes of  $\sigma_{ij}''-w_j$  and  $\sigma_{ij}'-w_j$  curves to obtain  $\tau_j$ 's appears to be reliable as it avoids polar-polar interaction unlike the linear slope of  $\sigma_{ij}''-\sigma_{ij}'$  curves. The appearance of peak in  $\sigma_{ij}-w_j$  and  $\sigma_{ij}''-w_j$  curves at different  $t$   $^{\circ}\text{C}$  for systems I and II indicates the change of phase of lower conductivity as  $w_j$  increases. *O*-chloroacetophenone, on the other hand, showed the monotonic increase of  $\sigma_{ij}$  and  $\sigma_{ij}''$  with  $w_j$ 's at all the temperatures. The temperature dependence the of  $\mu_j$ 's and  $\tau_j$ 's although they are measured in the limit of  $w_j=0$  supports this behaviour.  $\tau_j$  is zero for *m*-diisopropylbenzene at 54.03  $^{\circ}\text{C}$  while *p*-methylbenzoylchloride at 16.22  $^{\circ}\text{C}$  and 63.88  $^{\circ}\text{C}$  respectively indicating orderness at those temperatures. *o*-chloroacetophenone showed  $\tau_j$ 's decreasing with temperature and becomes zero at  $t=\infty$ . The corresponding  $\mu$ 's are  $\mu_s=13.80\times 10^{-30}$  C.m for *m*-diisopropylbenzene and  $\mu_s=9.07\times 10^{-30}$  C.m and  $\mu_s=10.47\times 10^{-30}$  C.m for *p*-methylbenzoylchloride respectively as static  $\mu_s$ . Both  $\tau_j$ 's and  $\mu_j$ 's in tables and figures are within 10% and 5% accuracies. The increase or decrease of  $\mu_j$ 's with temperature  $t$  in  $^{\circ}\text{C}$  is explained by asymmetric or symmetric configurations of the molecules. The energy parameters from  $\ln(\tau_j T)$  against  $1/T$  with  $\tau_j$ 's from the ratio of individual slopes of  $\sigma_{ij}''-w_j$  and  $\sigma_{ij}'-w_j$  curves at various temperatures indicate the stability of random dipole orientations in the activated states. The deviation of  $\mu_{theo}$  from the bond angles and bond moments of polar groups of molecules from measured  $\mu_j$  in terms of  $\tau_j$  can be explained by inductive, mesomeric and electromeric effect. The correlation between the conformational structures with the observed results enhances the scientific contents and adds a new horizon of understanding to the existing knowledge of dielectric relaxation.

#### References :

- [4.1] K V Gopalakrishna, *Trans. Faraday Soc.* **53** 767 (1957)
- [4.2] S N Sen and R Ghosh, *Indian J. Pure & Appl. Phys.* **10** 701 (1972)
- [4.3] U Saha, S K Sit, R C Basak and S Acharyya, *J. Phys. D: Appl. Phys.* **27** 596 (1994)
- [4.4] S K Sit, R C Basak, U Saha and S Acharyya, *J. Phys. D: Appl. Phys.* **27** 2194 (1994)
- [4.5] S K Sit and S Acharyya, *Indian J. Pure & Appl. Phys.* **34** 255 (1996)
- [4.6] N Paul, K P Sharma and S Chattopadhyay, *Indian J. Phys.* **71B** 711 (1997)

- [4.7] R C Basak, A Karmakar, S K Sit and S Acharyya, *Indian J. Pure & Appl. Phys.* **37** 224 (1999)
- [4.8] A K Jonscher, *Inst. Phys. Conf. Serial No. 58*, Invited paper presented at Physics of Dielectric Solids **8** (1980)
- [4.9] N Ghosh, R C Basak, S K Sit and S Acharyya, *J. Molecular Liquids* **85** 375 (2000)
- [4.10] M B R Murthy, R L Patil and D K Deshpande, *Indian J. Phys.* **63B** 491 (1989)
- [4.11] H Eyring, S Glasstone and K J Laidler, *Theory of Rate Processes* (McGraw Hill: New York) (1941)
- [4.12] S K Sit, N Ghosh, U Saha and S Acharyya, *Indian J. Phys.* **71B** 533 (1997)
- [4.13] C P Smyth, *Dielectric Behaviour and Structure* (McGraw Hill: New York) (1955)
- [4.14] A K Chatterjee, U Saha, N Nandi, R C Basak and S Acharyya, *Indian J. Phys.* **66B** 291 (1992)
- [4.15] S K Sit and S Acharyya, *Indian J. Phys.* **70B** 19 (1996)
- [4.16] M A El shahawy, A F Mansour and H A Hashem, *Indian J. Pure & Appl. Phys.* **36** 78 (1998)
- [4.17] A M Ras and P Bordewijk, *Recuel* **90** 1055 (1971)
- [4.18] “*Internal Rotation in Molecules*”- Edited by W J Orville Thomas (John Wiley) (1974)